Energy harvesting properties of all-thin-film multiferroic cantilevers

Tiberiu-Dan Onuta,[1,a)] Yi Wang,[2] Christian J. Long,[2] and Ichiro Takeuchi[1]
[1]*Department of Materials Science and Engineering, University of Maryland, College Park, Maryland 20742, USA*
[2]*Department of Physics, University of Maryland, College Park, Maryland 20742, USA*

(Received 7 September 2011; accepted 24 October 2011; published online 18 November 2011)

We have measured electromagnetic energy harvesting properties of all-thin-film magnetoelectric (ME) heterostructures on Si cantilevers. The devices are built on a silicon oxide/nitride/oxide stack, and the ME layers consist of a magnetostrictive $Fe_{0.7}Ga_{0.3}$ thin film and a $Pb(Zr_{0.52}Ti_{0.48})O_3$ piezoelectric thin film. The harvested peak power at 1 Oe is 0.7 mW/cm^3 (RMS) at the resonant frequency (3.8 kHz) with a load of 12.5 kΩ. The resonant frequency was found to display DC bias magnetic field dependence indicative of a magnetization canting with respect to the cantilever easy axis as a result of interplay between the anisotropy and Zeeman energies. © *2011 American Institute of Physics*. [doi:10.1063/1.3662037]

Self-powered sensor nodes are used in a wide spectrum of wireless applications ranging from *in vivo* encapsulated implants to industrial process monitoring.[1–3] In such applications, there is an acute need for development of low-cost alternative power sources without traditional batteries, which are undesirable for long-term critical power needs, maintenance-free applications, and for microsystems. To this end, energy harvesting from the environment has been actively explored using different physical principles. In particular, energy transfer by electromagnetic waves has great potential and can be accessible by using solenoid/piezoelectric-based transducers.[4]

The current surge of activities in multiferroic materials and structures has lead the way for development of a new generation of devices based upon magnetoelectric (ME) effects, where conversion of magnetic field (H) to electric field (E) takes place at the interface.[5–7] The ME composites based on bulk laminates have been demonstrated as power harvesters[1,8,9] operating at room temperature with high sensitivity. To date, reported wireless power receivers based on bulk ME devices consist of laminated layers of magnetostrictive/piezoelectric materials in cm-sized structures. However, such bulk ME laminate devices can be prone to shortcomings including (1) uneven and unreliable bonding between the magnetostrictive and the piezoelectric layer, which result in non-ideal coupling (and, in turn, low transduction efficiency), (2) high eddy current losses, and (3) low quality factor Q.

As an alternative technology, we are developing highly efficient miniaturized energy harvesters using all-thin-film ME structures on Si-micromachined cantilevers. We have previously reported on such micro-electromechanical systems (MEMS)-based devices demonstrating flexible platforms for fabrication of magnetic field sensors.[5] Miniaturized cantilever devices have advantages in making array-like sensor networks and ease of integration with peripheral circuits.

Our devices consist of free-standing $Pb(Zr_{0.52}Ti_{0.48})O_3$ (PZT)/magnetostrictive $Fe_{0.7}Ga_{0.3}$ cantilevers. The thin-film heterostructure is fabricated on a Si substrate with a plasma-enhanced chemical vapor deposited (PECVD) silicon oxide/nitride/oxide (ONO) stack. A 20-nm/100-nm Ti/Pt layer is sputtered at 430 °C to form the bottom electrode of the piezoelectric layer. A ~500-nm PZT layer is spun by a standard sol-gel process. The PZT layer is then covered by a 35-nm Pt buffer layer sputtered at 305 °C. A 500-nm $Fe_{0.7}Ga_{0.3}$ layer is then sputtered at room temperature. The Pt buffer layer between PZT and $Fe_{0.7}Ga_{0.3}$ layers serves to maintain robust adhesion of the films.

A central issue in fabricating cantilever-based devices is the film-stress engineering of the heterostructure.[10,11] We have developed a process of fabricating (~mm long) unbent cantilever beam structures using a 3.8-μm thick ONO stack with 6 layers of 75-nm low stress tensile-type silicon nitride separated by 100-nm silicon oxide layers. The neutral plane is at 2.9 μm with respect to the bottom of the heterostructure, outside the PZT layer. A four-mask photo-lithographic process is used to make the free-standing cantilevers 950-μm long and 200-μm wide shown in Fig. 1.

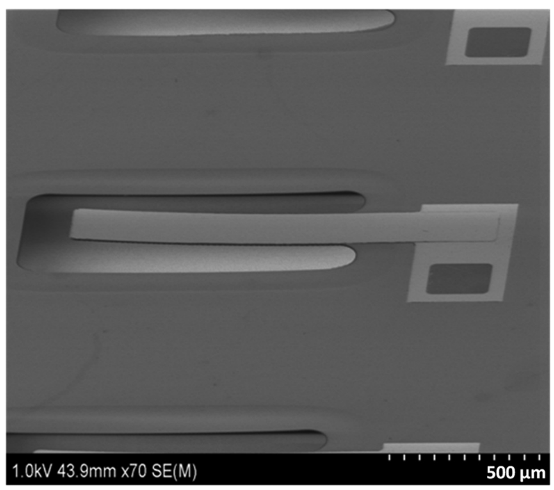

FIG. 1. A scanning electron micrograph (SEM) of a multiferroic energy harvester. The device is a 950-μm long and 200-μm wide released cantilever. The contact pads of the device to the bottom and upper electrodes are located at the root of the device.

[a)]Electronic mail: tonuta@umd.edu.

The ME characteristics of the devices relevant to the energy harvesting properties were measured in a set-up consisting of two pairs of Helmholtz coils (for AC and DC co-aligned magnetic fields). The device chip (6.6 mm × 6.6 mm) containing six cantilever devices was mounted in a vacuum chamber placed between the coils, and it was aligned parallel to the magnetic fields. The ME devices were initially poled at 5 V for 5 min. In dynamic measurements, the energy harvesting ME device was connected to a Stanford SR 830 DSP lock-in amplifier for induced voltage measurements while an AC magnetic field was applied, and both the AC field frequency and the DC magnetic field were swept. Different loads R_{load} were attached for energy harvesting measurements. All experiments were carried out at room temperature and vacuum of 3.5×10^{-4} mbar.

The mechanical resonant frequency of the fabricated cantilevers of length L can be best calculated using a bilayer model[12] that involves reducing all non-piezoelectric layers from the heterostructure to one equivalent electromechanically passive layer (called reduced layer) and an unreduced piezoelectric layer. The expression of the resonant frequency of the first bending mode based on this model is

$$f_{R0} = \frac{\lambda_1^2}{2\pi L^2}\left(\frac{E_{PZT}}{t_{PZT}\rho_{PZT} + t_{red}\rho_{red}}\right)^{\frac{1}{2}} \times \left[\frac{At_{red}^3}{12} + \frac{t_{PZT}^3}{12} + \frac{At_{red}t_{PZT}}{4}\cdot\frac{(t_{red}+t_{PZT})^2}{At_{red}+t_{PZT}}\right]^{\frac{1}{2}}, \quad (1)$$

where $\lambda_1 = 1.87$ is the eigenvalue of the first bending mode, t_{PZT} and ρ_{PZT} are the thickness and the density of the PZT layer, $t_{red} = \sum_{i=1}^{N} t_i$ is the total thickness of all films except the PZT layer, $\rho_{red} = \frac{1}{t_{red}}\sum_{i=1}^{N}\rho_i$ and $E_{red} = \frac{1}{t_{red}}\sum_{t=1}^{N}E_i$ are the density and the effective Young's modulus of the reduced layer, respectively, and $A = E_{red}/E_{PZT}$. An estimate of the resonant frequency based on the formula (1) gives us a value of 3.5 kHz. This is in good agreement with the measured values for over a set of 10 devices (3.75 kHz ± 5.5%).

Fig. 2 shows the results of energy harvesting measurements from a single all-thin-film multiferroic device. The device was biased with a 66.1 Oe DC magnetic field. This value was chosen in the region with highest ME voltage signals discussed below, and the AC field was applied at the resonant frequency of $f_R = 3833.1$ Hz. The multiferroic device is in the g_{31} mode of operation. The AC magnetic field was maintained at 1 Oe RMS. The voltage output from the harvesting devices saturates as a function of the external load (Fig. 2). The power output ($P = V_{RMS}^2/R_{load}$) has a peak that occurs for a load impedance of 12.5 kΩ. This experimental peak impedance value is consistent with the fact that impedance matching occurs at the optimal value of $R_{load} = 1/(2\pi f_{R0}C_0)$, where C_0 is the effective capacitance of the device (measured to be $C_0 = 3.2 \times 10^{-9}F$). To determine the power density of the multiferroic harvester, an effective volume ($950\,\mu m \times 200\,\mu m \times 0.5\,\mu m$) taking into account the freestanding length of the cantilever and the thickness of the poled (PZT) piezoelectric film was used. The measured peak power density is 0.7 mW/cm^3 (RMS). This value is similar to other reported harvested power densities of bulk laminate devices at 1 Oe (RMS).[1,9]

Fig. 3 shows the AC magnetic field dependence of the harvested voltage and power for a 12.5 kΩ load and a DC bias of 66.1 Oe. The saturation plateau in both power and voltage with respect to increasing AC magnetic field is due to the saturation of the internal stress of magnetic origin that involves the rotation of magnetization vector.

We have found that the resonant frequency of the present ME devices exhibit strong dependency on the magnitude and the sweeping direction of the DC bias field (H) (Figs. 4(a) and 4(b)). This indicates that the resonant frequency of the first-order flexural mode of the devices is determined not only by the mechanical properties of the devices, but also by the magnetic properties. The discontinuity in the DC field dependence of the resonant frequency occurs at 77 Oe (Fig. 4(c)). This value agrees with the coercive field of the 500-nm thick $Fe_{0.7}Ga_{0.3}$ films measured by vibrating sample magnetometry (VSM). A similar behavior was previously observed both in nano-electromechanical systems (NEMS) based devices[13] and in larger clamped beams.[8,14] From Fig. 4(b), one sees that the highest ME coefficient of this device

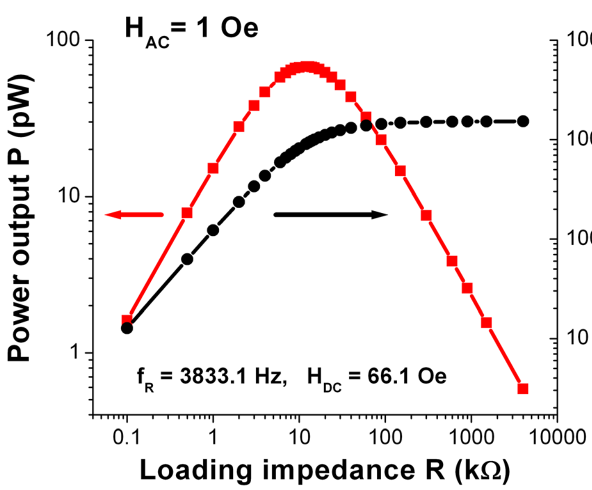

FIG. 2. (Color online) Energy harvested RMS voltage at bias field $H_{DC} = 66.1$ Oe and corresponding resonant frequency of 3833.1 Hz. Also, one displays the raw power measured as a function of loading impedance at resonance. The harvested AC magnetic field is $H_{AC} = 1$ Oe RMS.

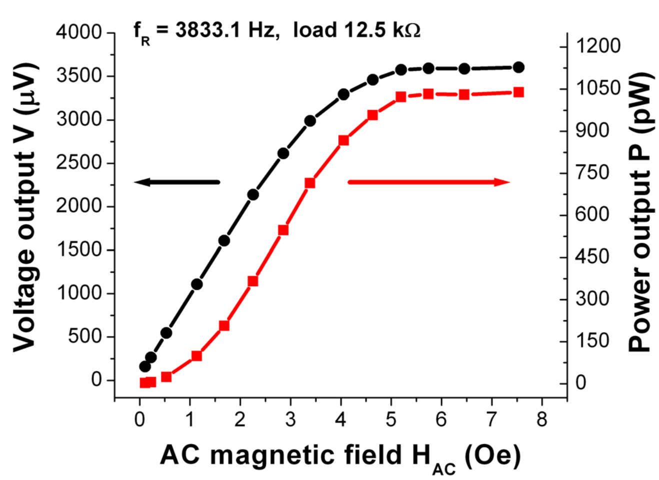

FIG. 3. (Color online) Dependence of the output voltage and raw harvested power on the AC magnetic field at resonance. The bias field is $H_{DC} = 66.1$ Oe. The load is 12.5 kΩ, corresponding to the peak power from Fig. 2.

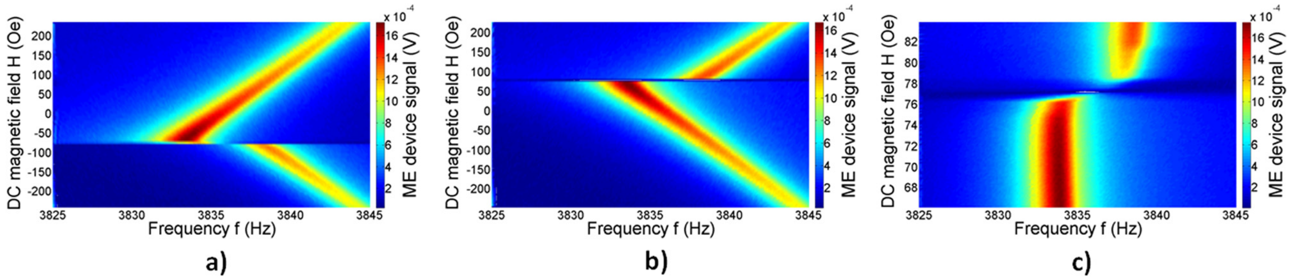

FIG. 4. (Color online) DC magnetic field (H) dependence of the multiferroic energy harvester resonant frequency with 1 Oe AC magnetic field. (a) DC field is swept from 238 to −238 Oe. (b) DC field is swept in opposite direction from −238 to 238 Oe. (c) A close-up of the magnetization switching region taken from (b).

is $33.6V/(cm \cdot Oe)$, and it is when the DC bias field is 66.1 Oe which "sets" $f_R = 3833.1$ Hz. Also, the Q-factor of the device is ≈2000 and has a pronounced dependence on the DC bias magnetic field. An interesting consequence of the field dependent f_R is that as seen in Figs. 4(a) and 4(b)), the device can be operated at zero DC magnetic bias field with a relatively high ME coefficient as long as the AC field frequency is at the $f_R(H=0)$. In fact the ME coefficient at zero bias field is only about 20% less than that when the bias field is close to the coercive field of the $Fe_{0.7}Ga_{0.3}$ film. Removing the necessity to apply DC bias significantly simplifies the operation setup of these devices for both magnetic field sensing and energy harvesting schemes.

To explain the bias field dependence of the resonant frequency of our devices, we adopt a model previously used to describe the behavior of magnetic cantilevers in Ref. 15. It is based on the competition of both magnetic anisotropy energy ($K_u V \sin^2\theta$) and Zeeman energy ($HM_sV\cos(\beta-\theta)$) of the $Fe_{0.7}Ga_{0.3}$ film to the canting of the resultant magnetization of the film with respect to its easy axis (where K_u is the anisotropy, V is the volume of the $Fe_{0.7}Ga_{0.3}$ film, H is the applied DC field, M_s is the saturation magnetization, β is the cantilever angle with respect to the field direction, and θ is the angle of the magnetization canting due to the external DC field). Both the total film energy with respect to θ and the generation formalism of a restoring torque by the resultant film magnetization vector are minimized within small angle approximation. It is shown that the occurrence of torque stiffens the cantilever spring constant. The overall effect can be expressed as[15]

$$f_R = \left(\frac{mHH_k}{2k_0 L_e^2 (H+H_k)} + 1\right) f_{R0}, \tag{2}$$

where f_R is the shifted resonant frequency due to the presence of an external DC magnetic field with respect to the natural resonance f_{R0}. We take the effective cantilever length ($L/L_e = 1.38$) for the first flexural mode[15] to be $L_e = 0.035\,cm$. The calculated spring constant is $k_0 = 2220\,g/s^2$, and $m = M_sV$. If we take into account the VSM-measured magnetic moment of $m \sim 500\ \mu emu$, and the overall magnetostrictive film volume of $\sim 6 \times 10^{-7}$ cm^3 (corresponding to six cantilevers on the device chip), then the experimental saturation becomes $M_s \sim 833.3\ emu$/cm^3 for $Fe_{0.7}Ga_{0.3}$. The anisotropy field H_k is used as the parameter to fit the experimental f_R-H curve (taken from a single device) to expression (2). For a device model parameter of $m \sim 90\ \mu emu$, the obtained value of the anisotropy field is $H_k = 307\,Oe$. This in turn gives the anisotropy $K_u = (M_s \times H_k)/2$ to be $K_u = 1.4 \times 10^5 (emu \times Oe)/cm^3$. A separately determined K_u from VSM measurements of $Fe_{0.7}Ga_{0.3}$ gives $K_u = 8.4 \times 10^4 (emu \times Oe)/cm^3$. The agreement of these values of K_u indicates that this model is adequate in explaining the experimental behavior of devices.

This work was supported by DARPA HUMS program (DARPA DSO FA86500917944), and partially supported by ARO W911NF-07-1-0410, UMD-NSF-MRSEC (DMR 0520471), and NEDO. Fabrication was performed at the Cornell Nano-Scale Science and Technology Facility (CNF) and at the Maryland Nanocenter Fablab. SEM images were taken at the NISP Lab of Maryland Nanocenter. We acknowledge Vince Genova, Sam Lofland, Peng Zhao, Luz Sanchez and Ron Polcawich for valuable discussions.

[1]R. C. O'Handley, J. K. Huang, D. C. Bono, and J. Simon, IEEE Sens. J. **8**, 57 (2008).
[2]H. U. Kim, W. H. Lee, H. V. R. Dias, and S. Priya, IEEE Trans. Ultrason. Ferroelectr. Freq. Control **56**, 1555 (2009).
[3]S. Priya, J. Ryu, C. S. Park, J. Oliver, J. J. Choi, and D. S. Park, Sensors **9**, 6362 (2009).
[4]L. X. Bian, Y. M. Wen, P. Li, Q. L. Gao, and M. Zheng, Sens. Actuators, A **150**, 207 (2009).
[5]P. Zhao, Z. L. Zhao, D. Hunter, R. Suchoski, C. Gao, S. Mathews, M. Wuttig, and I. Takeuchi, Appl. Phys. Lett. **94**, 243507 (2009).
[6]H. Greve, E. Woltermann, R. Jahns, S. Marauska, B. Wagner, R. Knochel, M. Wuttig, and E. Quandt, Appl. Phys. Lett. **97**, 152503 (2010).
[7]H. Greve, E. Woltermann, H. J. Quenzer, B. Wagner, and E. Quandt, Appl. Phys. Lett. **96**, 182501 (2010).
[8]P. Finkel, S. E. Lofland, and E. Garrity, Appl. Phys. Lett. **94**, 072502 (2009).
[9]S. X. Dong, J. Y. Zhai, J. F. Li, D. Viehland, and S. Priya, Appl. Phys. Lett. **93**, 103511 (2008).
[10]Y. B. Jeon, R. Sood, J. H. Jeong, and S. G. Kim, Sens. Actuators, A **122**, 16 (2005).
[11]J. S. Pulskamp, A. Wickenden, R. Polcawich, B. Piekarski, M. Dubey, and G. Smith, J. Vacuum Sci. Technol. B **21**, 2482 (2003).
[12]Q. M. Wang and L. E. Cross, J. Appl. Phys. **83**, 5358 (1998).
[13]H. Bhaskaran, M. Li, D. Garcia-Sanchez, P. Zhao, I. Takeuchi, and H. X. Tang, Appl. Phys. Lett. **98**, 013502 (2011).
[14]P. Finkel, J. Bonini, E. Garrity, K. Bussman, J. Gao, J. F. Li, S. E. Lofland, and D. Viehland, Appl. Phys. Lett. **98**, 092905 (2011).
[15]B. C. Stipe, H. J. Mamin, T. D. Stowe, T. W. Kenny, and D. Rugar, Phys. Rev. Lett. **86**, 2874 (2001).